Kidney International, Vol. 59 (2001), pp. 1803–1811

ION CHANNELS – MEMBRANE TRANSPORT – INTEGRATIVE PHYSIOLOGY

Functional heterogeneity of ROMK mutations linked to hyperprostaglandin E syndrome

Nikola Jeck, Christian Derst, Erhard Wischmeyer, Henning Ott, Stefanie Weber, Christoph Rudin, Hannsjörg W. Seyberth, Jürgen Daut, Andreas Karschin, and Martin Konrad

Department of Pediatrics and Institute of Physiology, Philipps-University, Marburg, and Max Planck-Institute for Biophysical Chemistry, Göttingen, Germany; and University Children's Hospital, Basel, Switzerland

Functional heterogeneity of ROMK mutations linked to hyperprostaglandin E syndrome.

Background. The renal K^+ channel ROMK (Kir1.1) controls salt reabsorption in the kidney. Loss-of-function mutations in this channel cause hyperprostaglandin E syndrome/antenatal Bartter syndrome (HPS/aBS), which is characterized by severe renal salt and fluid wasting.

Methods. We investigated 10 HPS/aBS patients for mutations in the *ROMK* gene by single-strand conformation polymorphism analysis (SSCA) and direct sequencing. To assess the functional consequences, Ba^{2+}-sensitive K^+ currents were measured in five mutants of the core region as well as one mutant with truncated C-terminus, using the two-electrode voltage-clamp technique after an injection of mutant cRNA into *Xenopus* oocytes.

Results. Three novel ROMK mutations were identified together with six mutations described previously. The mutations were categorized into three groups: (*1*) amino acid exchanges in the core region (M1-H5-M2), (*2*) truncation at the cytosolic C-terminus, and (*3*) deletions of putative promoter elements. While the core mutations W99C, N124K, and I142T led to significantly reduced macroscopic K^+ currents (1 to 8% of wild-type currents), the A103V and P110L variants retained substantial K^+ conductivity (23 and 35% of wild-type currents, respectively). Coexpression of A103V and P110L, resembling the compound heterozygous state of the affected individual, further reduced macroscopic currents to 9% of the wild-type currents. All mutants in the core region exerted a dominant-negative effect on wild-type ROMK1. The C-terminal frameshift (fs) mutation (H354fs) did not change current amplitudes compared with ROMK1 wild type, suggesting that a mechanism other than alteration of the electrophysiological properties may responsible for loss of channel activity.

Conclusions. Analysis of ROMK mutants linked to HPS/aBS revealed a spectrum of mechanisms accounting for loss of channel function. Further characterization of the molecular defects might be helpful for the development of new therapeutic approaches.

Key words: K^+ channel, channelopathy, antenatal Bartter syndrome, *KCNJ1* gene, renal fluid wasting, salt reabsorption.

Received for publication August 3, 2000
and in revised form November 6, 2000
Accepted for publication November 13, 2000

Transport of potassium ions (K^+) through the renal epithelia plays a key role in potassium balance [1]. Furthermore, secretion of K^+ from the epithelial cell into the tubular lumen is essential for NaCl reabsorption via the Na-K-2Cl cotransporter in the thick ascending loop of Henle (TAL) [2]. Efforts to identify molecules responsible for renal K^+ secretion led to cloning of the ROMK channel (renal outer medullary K^+ channel; also termed Kir1.1) [3]. Three ROMK isoforms have been identified, with ROMK1 and ROMK3 having their N-termini extended by 19 and 17 residues, respectively, as compared with ROMK2 [4]. The rat homologues are expressed differentially along the loop of Henle and the distal nephron [5]. Mutations in the ROMK channel gene, *KCNJ1*, result in hyperprostaglandin E syndrome/antenatal Bartter syndrome (HPS/aBS) [6, 7], thereby indicating the importance of ROMK for salt reabsorption in the TAL. Affected individuals possess the typical pattern of impaired TAL function, including saliuretic polyuria, impaired urine concentration ability, and hypercalciuria [8, 9].

ROMK belongs to a family of structurally and functionally related K^+ channels designated as Kir channels [10]. Kir channels are assembled from four subunits. Hydropathy and sequence analyses predict cytoplasmic N- and C-termini with a well-conserved core region, which consists of two transmembrane helices, M1 and M2, flanking a pore-forming H5 segment containing the selectivity filter for potassium ions (G-Y/F-G-motif) and a flexible linker region between M1 and H5 [3]. ROMK subunits form homotetrameric assemblies. However, heterotetrameric assemblies together with Kir4.1 (also designated as Kir1.2) and Kir4.2 (also designated as Kir1.3) subunits have also been reported [11, 12]. In addition, it has been suggested that ROMK interacts with cystic fibrosis transmembrane conductance regulator (CFTR), a member of the ATP binding cassette (ABC)-transporter family, to form adenosine 5′-triphosphate (ATP)-sensitive potassium channels in renal epithelial cells [13].

Kir channels are characterized by their ability to conduct K^+ more readily in the inward than the outward direction. ROMK is a weakly rectifying K^+ channel and is gated by intracellular pH with acidification leading to channel closure [14]. A molecular triad composed of the intracellular residues R41-K80-R311 was found to be a prerequisite for channel gating at physiological pH [15].

Recent analysis of the functional consequences of naturally occurring mutations in HPS/aBS contributed much to the understanding of ROMK physiology. All point mutations linked to HPS/aBS were found in exon 5, which encodes the main part of the protein and is common to all ROMK isoforms. Thus, all ROMK channels along the nephron will be affected by the mutations. When expressed in COS-7 cells, ROMK variants harboring mutations in the core region showed no significant macroscopic potassium currents, whereas mutations occurring in the N- and C-termini infrequently expressed very low current levels [16]. The dominant-negative N124K mutation in the linker region between M1 and the H5 region was found to abolish the expression of functional channels, suggesting an important role of this residue for channel assembly [12]. Two C-terminal mutations, which were located nearby or inside the putative protein kinase A (PKA) phosphorylation site at position S219, showed a decreased open probability of the channel either by accelerating channel rundown or by inducing long closed states [17, 18]. Recently, several mutations located in the intracellular N- and C-termini were shown to alter pH-dependent gating [15]. Most of these mutants encoded functional channels, but their pH gating was shifted to more alkaline pH values. These shifts in pH gating are proposed to result from disruption of the R41-K80-R311 triad or from mutation-induced structural disturbances of this arrangement.

Our study describes three novel mutations in ROMK, along with six mutations reported previously. Six mutant variants were electrophysiologically characterized. Taking previous findings into consideration, analyses of naturally occurring ROMK mutations revealed distinctly different mechanisms related to loss of channel function.

METHODS

Patients

Mutational analysis was performed in 10 patients diagnosed for HPS/aBS following the criteria of Seyberth et al [9]. Laboratory data were obtained from the hospital records. Prior to enrollment in the study, the *SLC12A1* gene encoding NKCC2 was excluded as a disease-causing gene by either haplotype analysis or single-strand conformation polymorphism analysis (SSCA). This study was approved by the local ethics committee, and informed consent was obtained from the patients and/or their parents.

Mutational analysis

Genomic DNA of all affected individuals and available family members was extracted from whole blood using standard methods [19]. Previously reported primer pairs and polymerase chain reaction (PCR) conditions were applied for amplification of the coding region of *KCNJ1* [7]. For amplification of the promoter region and exons 1 to 3 of *KCNJ1*, four additional primer pairs were designed (Table 1).

The *KCNJ1* gene was screened for mobility shifts by SSCA [20]. Electrophoretic separation of the single-strand DNA was performed in a 10% polyacrylamide gel (Clean Gel; Pharmacia Biotech, Quebec, Canada) using the Multiphor II electrophoresis system (Pharmacia Biotech) with 18 W constant power for one hour at two temperatures, 9°C and 15°C. The band patterns were visualized using the silver staining method (Plus-One DNA silver staining kit; Amersham Pharmacia, Arlington Heights, IL, USA). Direct sequencing was performed after reamplification of the remaining PCR product using 5′-Cy5–labeled primers on the ALF express sequencing system (Pharmacia Biotech) following the protocols provided by the manufacturer. DNA sequences were confirmed by sequencing both strands from the patient, the parents, and a healthy control. Mutations were discerned from innocuous polymorphisms by demonstration of their absence in 100 control alleles.

To detect the cytosine insertion at nucleotide 1116 (according to GenBank™ U12541), we designed a mutagenic reverse primer (5′-ATAAAGGCACATGGCACAGT GACGG-3′, T_{aneal} 66°C) introducing a cleavage site for the endonuclease *Asp I* (Boehringer Mannheim, Mannheim, Germany) in the mutant allele but not in the wild type. After digestion of the PCR product at 37°C for three hours, the samples were applied on a 10% polyacrylamide gel, separated in the electric field (600 V, 18 W) and subsequently silver stained.

Haplotype construction

Haplotype construction was performed using four polymorphic markers closely linked to the *KCNJ1* locus on chromosome 11q24-25 (D11S912, D11S4150, D11S4131, D11S910). Haplotype analysis followed previously published protocols [7].

Mutagenesis and expression system

For expression in *Xenopus* oocytes, the human ROMK1 cDNA cloned into the polyadenylating oocyte-expression vector pSGEM (a gift of M. Hollmann, Göttingen, Germany) was used. Site-directed mutagenesis was performed using 25-mer oligonucleotide primers with the engineered nucleotide changes in the center of the primer (leading to amino acid changes W99C, A103V, P110L, N124K, I142T, and H354fs) and a commercial kit (Quik

Table 1. Primer pairs and annealing temperatures for analysis of the 5′ part of *KCNJ1*

	Forward primer (5′→3′)	Reverse primer (5′→3′)	T_{anneal}
KCNJ1 5′	CATCCCATATTCATTATTTCATTC	CCCAAGGAGCCCCTCACAAA	60°
KCNJ1 exon 1	CACGCCTACTCTTGTTGGAT	CGGGGAAAAGAGGTCTAAAT	63°
KCNJ1 exon 2	TTACCTTCACCCAAATGTCTT	CGTCTATGCACCAAATCTGT	63°
KCNJ1 exon 3	GTGGGCCTGTCCTCTGTCTC	AGCCTGGGGTGTCCAATAGT	63°

Change™; Stratagene, La Jolla, CA, USA) as described by the manufacturer. The entire ROMK1 coding region was sequenced in order to confirm that only the intended nucleotide exchange had occurred. Capped run-off cRNA polyA+ transcripts were synthesized from linearized cDNA using T7-RNA polymerase and injected in defolliculated oocytes. Three nanograms cRNA were injected for the expression of wildtype or mutant channels alone. For coexpression of wild-type and mutant subunits, equivalent amounts of cRNA (3 ng cRNA each) were injected, allowing a comparison of whole cell currents from coinjected oocytes and oocytes expressing wild-type or mutant ROMK alone. Oocytes were incubated at 20°C in ND96 solution (96 mmol/L NaCl, 2 mmol/L KCl, 1 mmol/L $MgCl_2$, 1 mmol/L $CaCl_2$, HEPES, pH 7.4) supplemented with 100 μg/mL of gentamycin and 2.5 mmol/L sodium pyruvate. Electrophysiological measurements were performed 48 hours after injection.

Electrophysiological procedures

Two-electrode voltage-clamp measurements were performed as described earlier [12] using a Turbo Tec-10 C amplifier (*npi*; Germany) and sampled through an EPC9 interface (Heka Electronics, Lamprecht, Germany) using PULSE/PULSEFIT software for data acquisition and IGOR software for data analysis.

RESULTS

Patients

The patient cohort consisted of three offspring of consanguineous unions and seven sporadic cases. In each case, both mutant alleles have been identified. The genetic data and the corresponding phenotypes are summarized in Table 2. The phenotype of patient V has been reported previously [9, 21, 22]. All patients were born prematurely with a median gestational age of 32 weeks. Postnatally, renal salt losses led to a drop of plasma sodium to a minimum value of 125 mmol/L (median). Three out of 10 patients exhibited transitory, marked hyperkalemia (plasma K^+ levels >7 mmol/L) in the neonatal period. During follow-up, eight patients developed hypokalemic alkalosis secondary to hyperaldosteronism. The time of onset of hypokalemic alkalosis varied considerably from one week up to five years of age. In patients IV and VII, hypokalemic alkalosis was not observed at any time. The median minimal potassium level recorded in the patients' follow-up was 3.0 mmol/L. The patients' ability to produce concentrated urine was severely impaired, and urinary calcium persisted at high levels. Eight out of 10 patients were treated with the cyclooxygenase inhibitor indomethacin with beneficial effects in terms of reduction of saliuretic polyuria, partial or complete resolution of hypokalemia, a decrease of urinary calcium excretion, and better growth.

Genetics: Missense mutations

Two novel missense mutations were identified (I and II) together with four missense mutations previously described in HPS/aBS patients (III through VI; Table 2). The novel point mutations represent an exchange from alanine-103 to valine and from isoleucine-142 to threonine. A103 is located in the transmembrane domain M1, and I142 is directly adjacent to the selectivity filter in the pore region. Both residues are highly conserved within the Kir family.

Three additional missense mutations detected in our patients affect the core region of the K^+ channel: The W99C mutant alters the M1 domain, while P110L and N124K alter the extracellular linker between M1 and H5. Only one missense mutation was found in the intracellular C terminus, substituting glycine for valine at codon 315.

Nonsense mutations

Two patients (VI and VII) were found to carry a 4 bp deletion spanning the last base of codon T332 and all of codon K333. This mutation was previously described in two unrelated HPS/aBS patients [6, 7]. Since a relationship between these families was not apparent, the high prevalence of this mutation may reflect a particular susceptibility of this genomic site.

We originally failed to detect the second disease-causing mutation in three patients (III through V). Therefore, direct sequencing of the coding region of *KCNJ1* was performed. All three patients turned out to carry the same insertion of a single cytosine base in a polycytosine tract spanning codons 352 and 353, resulting in a frameshift mutation and altering the encoded protein from amino acid 354 onward, ending at a new stop codon at position 362. As we missed this mutation by our SSCA screening, we designed a mutagenic reverse primer introducing an *Asp I* cleavage site in the mutant allele. Subsequent digestion of the PCR product then enabled us to detect the three patients together with one additional patient

Table 2. Genetic and phenotypic characteristics of ten HPS/aBS patients enrolled into the study

Patient	Mutation	Age at diagnosis/ major clinical signs	Polyhydramnios/ gestational age *weeks*	Min. Na^+ level (*mmol/L*)/ Na^+ suppl. (*mmol/kg/day*)	Max. K^+ level[d]	Min. K^+ level	Urinary osmolality *mmol/kg*	Hypercalciuria *mg/kg/day*
					mmol/L			
I	**A103V** P110L	4 years/nephrocalcinosis	−/33	128/7	5.4	3.3	285–431	13
II	**I142T** P110L	2 months/hypokalemia, hyponatremia, nephrocalcinosis	+/30	116/ND	9.4	2.3	180–318	Ca/Crea (*mol*) 3
III	W99C **1116insC→362X**	1 month/polyuria, hyponatremia	+/35[c]	132/10	5.2	3.1	107–236	7.8
IV	N124K **1116insC→362X**	9 months/fever, nephrocalcinosis	+/28	ND/40	9	3.7	122–337	14
V	V315G **1116insC→362X**	8 months/dystrophia, fever	+/30	129/12	6.5	2.2	63–340	9.5
VI	V315G 1053delAAAG→368X	2 months/polyuria, hyponatremia	+/32	124/15	6.3	3.0	195	10.5
VII[a]	1053delAAAG→368X[b]	13 months/dystrophia	+/36	126/ND	4.4	3.8	<300	Ca/Crea (*mol*) 2.6
VIII	**1116insC→362X[b]**	2 months/hypokalemia, hyponatremia, nephrocalcinosis	+/29	124/ND	8.2	3.0	127–335	12.8
IX[a]	del ex1-2[b]	1 month/polyuria, hypokalemia	+/32	128/22	4.8	3.0	255–305	Ca/Crea (*mol*) 4.7
X[a]	del ex1-2[b]	1 month/polyuria, nephrocalcinosis	+/34	125/8	4.8	2.8	ND	25

Novel mutations are indicated by bold letters; nucleotides are numbered according to GenBank accession number U12541.
[a] Offsprings of consanguineous unions
[b] Homozygous
[c] Received indomethacin between 28 and 31 weeks of gestation
[d] Average of the three highest plasma K^+ values within the first four weeks of life

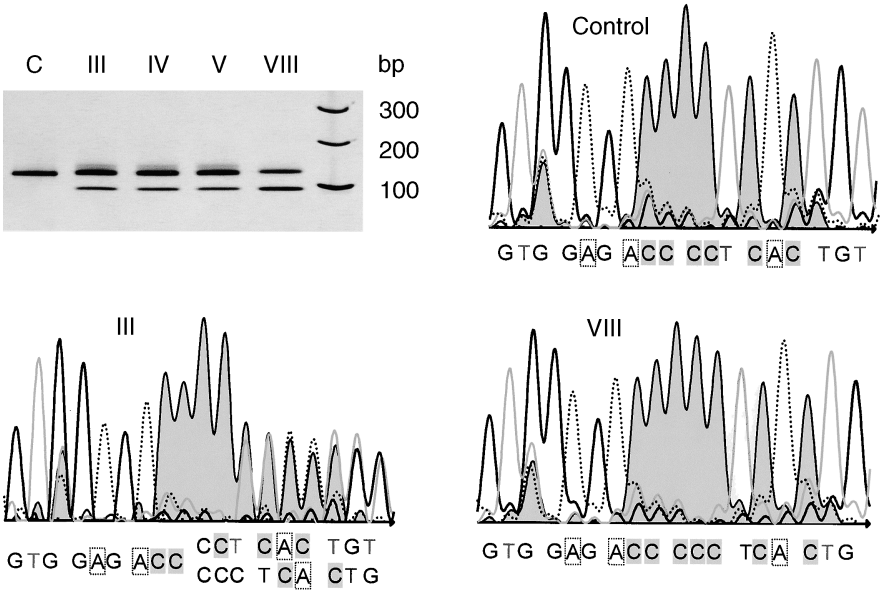

Fig. 1. Detection of a single cytosine insertion at residue P353. Electrophoretical separation of the "modified" polymerase chain reaction (PCR) fragments after digestion with *Asp I* in a 10% polyacrylamide gel. Only amplification products of the mutant allele were digested, leading to an additional band at 100 bp. In addition to the three heterozygotes, we detected a patient harboring this variant on both paternal alleles (VIII, digestion not complete). Direct sequencing of patients III and VIII confirms the cytosine insertion and the resulting frameshift (H354fs) in heterozygous and homozygous state, respectively.

(VIII) having a homozygous cytosine insertion (Fig. 1). This variant was not seen in 100 unaffected subjects.

The frequent insertion of a cytosine in a polycytosine tract [that is, $(C)_4$1112-15 according to GenBank accession number U12541] might reflect a susceptibility of this mononucleotide repeat tract to mutations from "slipped strand mispairing." On the other hand, because all patients carrying the cytosine insertion originated from Germany, the high frequency of this mutation may also be attributable to a founder effect. Indeed, four of five affected chromosomes share the same polymorphism with respect to the D11S4150 microsatellite, which is located next to *KCNJ1* (data not shown). Since the prevalence of this D11S4150 variant in the normal German population was found to be less than 5%, these results are suggestive for a common ancestor.

Deletion of exons 1 and 2

In two unrelated patients (IX and X), each of them having consanguineous parents, the haplotype data indicated linkage to the *KCNJ1* locus on chromosome 11p24 (data not shown). Since sequencing of exon 5 of the *KCNJ1* gene did not reveal any abnormality, we subsequently analyzed the isoform-specific exons 1 to 4 and the nearby transcription initiation sites. Amplification of exons 3 and 4 from the patients' genomic DNA resulted in PCR products of the predicted length. In contrast, we failed to obtain the respective PCR product for exons 1 and 2. Subsequent amplification using a primer pair (*KCNJ1* 5′) annealing almost 600 (forward) and 250 (reverse) bp upstream of exon 1 and, alternatively, using the same forward primer together with the reverse primer of exon 1 yielded no PCR product either, whereas products

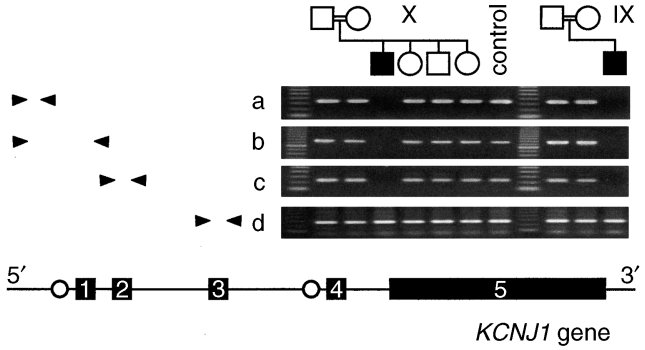

Fig. 2. Demonstration of the large deletion of the 5′ part of *KCNJ1*. (*Bottom*) Genomic organization of the *KCNJ1* gene, which consists of five exons, with exon 5 encoding the main part of the channel protein. Alternative splicing of exons 1 to 4 accounts for the generation of three protein isoforms. Two putative promoter elements *are located* in 5′ of exon 1 and exon 4, respectively (○). (*Left*) Arrowheads at the 5′ part of *KCNJ1* indicate the annealing sites for the primers used for deletion detection. (*Right*) PCR products from patients, family members, and a control separated on 1.5% agarose gel: (*a*) *KCNJ1* 5′, (*b*) *KCNJ1* 5′ (forward) together with *KCNJ1* exon 1 (reverse), (*c*) *KCNJ1* exon 2; *KCNJ1* exon 3 (Table 1).

of the predicted length were obtained in the parents and nonaffected siblings as well as in a control subject (Fig. 2). A similar finding has recently been reported by Feldmann, Alessandri, and Deschenes [23].

Electrophysiology

The electrophysiological properties of five mutations in the core region of ROMK1 (W99C, A103V, P110L, N124K, I142T) and a C-terminal frameshift mutation (H354fs) were analyzed by heterologous expression in *Xenopus* oocytes. When examined by two-electrode volt-

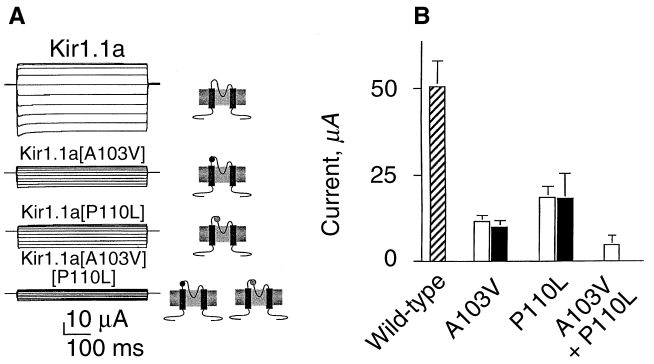

Fig. 3. Quantitative analysis of the two ROMK mutations A103V and P110L in *Xenopus* oocytes. (*A*) Original recordings show current responses of cRNA-injected oocytes to 500 ms voltage steps between 80 and −140 mV from a holding potential of 0 mV $[K^+]_e$ = 96 mmol/L. The inset diagrams illustrate the position of the two mutant residues in the extracellular M1-H5 linker of the ROMK subunit. (*B*) Steady-state current amplitudes derived from wild-type (▨) and mutant (□) channels and a combination of both (■) measured at −100 mV. When expressed alone, 3 ng cRNA of ROMK1 variants were injected. For coexpression, equimolar amounts of mutant or wild-type cRNA (3 ng each) were coinjected. Values are discussed in the text. Errors are mean ± SD.

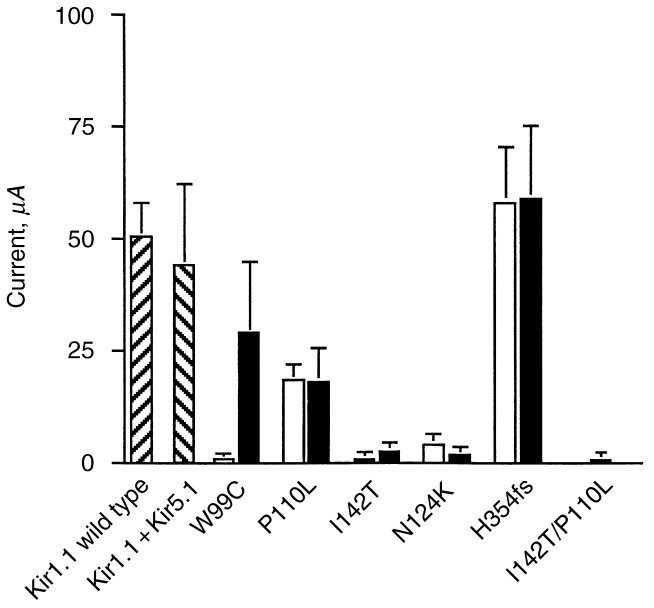

Fig. 4. Mean current amplitudes of wild-type and mutant ROMK channels in *Xenopus* oocytes. Amplitudes are steady-state currents generated by mutant and equimolar mutant/wild-type channels measured at −100 mV in 96 extracellular K^+. Figure 3 discussed the amounts of injected cRNAs. As a control, coexpression of the Kir5.1 subunit did not significantly change ROMK currents. Note that Kir5.1 has to assemble with Kir4.1 or Kir4.2 subunits for functional expression [24, 25]. Coexpression of wild-type and H354fs mutant did not result in a further increase in currents probably due to saturating amounts of cRNA injected. Symbols are: (■) mutant + wild-type; (□) mutant.

age-clamp, all mutant ROMK1 channels carrying the individual core mutation showed a significant but variable decrease in macroscopic inward currents when compared with wild-type ROMK1. With the extracellular K^+ concentration raised to 96 mmol/L, wild-type ROMK1 current amplitudes averaged −50.6 ± 8.0 μA (N = 9) at −100 mV membrane potential. In contrast, the two mutations present in patient I, A103V (−11.5 ± 2.7 μA, N = 9) and P110L (−18.5 ± 3.9 μA, N = 7), reduced macroscopic current amplitudes to 23 and 35%, respectively, under the same recording conditions (Fig. 3). When these ROMK1 mutants were coexpressed with equal amounts of wild-type cRNAs (100% each of control), macroscopic currents were not significantly different compared with the mutants alone (A103V/WT: −9.8 ± 2.6 μA, N = 7; P110:/WT: −17.9 ± 8.2 μA, N = 7), indicating a dominant negative effect. However, the expression of both mutant ROMK1 subunits together, mimicking the compound heterozygous state of patient I, resulted in macroscopic currents with significantly smaller amplitude than were found for either of the two mutations alone (A103V/P110L: −4.5 ± 2.2 μA, N = 10; 9% of wild-type current; Fig. 3).

Whole-cell currents of oocytes expressing ROMK1 channels carrying the mutations W99C (−0.8 ± 0.5 μA, N = 10), N124K (−3.9 ± 1.2 μA, N = 5), or I142T (−0.5 ± 0.4 μA, N = 10) were even more dramatically reduced to 2, 8, and 1%, respectively (Fig. 4). Interestingly, deficient W99C channels were partially rescued by wild-type ROMK1 (−29.1 ± 15.4 μA, N = 10; Fig. 4), whereas equimolar coinjection of wild-type ROMK1 cRNA did not significantly alter macroscopic current amplitudes of mutant N124K and I142T. In patient II (I142T/P110L), where both alleles were affected by mutations of the core region, channel function was likely to be severely impaired: macroscopic currents observed after coinjection of I142T/P110L averaged approximately 1% of the wild-type ROMK1 current (−0.6 ± 0.3 μA, N = 10). It should be noted that in all cases, quantitatively similar results have been obtained after transient channel expression in COS-7 cells (data not shown).

In contrast, expression of the C-terminal frameshift mutation (H354fs) in oocytes (and COS-7 cells, data not shown) did not result in decreased macroscopic currents when compared with wild type (−57.2 ± 17.8 μA, N = 10). This demonstrates that the electrophysiological properties of this mutation are unlikely to be responsible for the HPS/aBS phenotype.

DISCUSSION

This study confirms that mutations in the potassium channel ROMK are a common cause of HPS/aBS and, in addition, that the molecular defects underlying the loss of channel activity are heterogenous. Based on the functional consequences, three major classes of mutations were recognized in this study: (*1*) point mutations in the

core region, (*2*) truncating mutations in the C-terminus, and (*3*) deletions of putative promoter elements.

Mutations in the core region are either located in the highly conserved channel pore or in the less conserved M1-H5 linker region. In the hydrophobic M1 segment, the loss-of-function phenotype may be caused by introducing bulky (A103V) or polar (W99C) amino acids. Another possible mechanism is the impairment of the selectivity filter by changes of the residues adjacent to the GYG-motif (I142T). It is less clear, however, how mutations in the extracellular loop would disturb channel function (P110L, N124K). Our data on the P110L and N124K mutations together with previous results on a nearby mutation (D108H) [16] suggest that the tertiary structure of the entire extracellular loop, although not directly involved in pore formation, is essential for channel function. Thus, certain amino acid substitutions may be sterically incompatible with a functional pore structure. Indeed, a compact folding of the extracellular loop is supported by the crystal structure of the *Streptomyces lividans* K^+ channel [26].

Two mutants in the core region, A103V and P110L, retained substantial macroscopic potassium currents, which seemed to be inconsistent with their proposed pathogenic role at first sight. However, our HPS/aBS patients, as well as an additional one described previously [7], which were affected from the P110L exchange, were found to be compound heterozygotes, harboring a different mutation on the second parental allele. In the oocyte system, coexpression of the A103V and P110L mutants (a condition as in patient I) resulted in significantly smaller macroscopic currents as compared with the currents from each mutant separately. Possibly, the close proximity of the two residues gives rise to major structural changes in the linker region. Moreover, a combination of P110L with I142T (patient II) resulted in 20 times lower macroscopic currents as compared with P110L/A103V. The residual potassium conductance in P110L/A103V may account for the milder phenotype of patient I (Table 2). We therefore suggest that the combination of mutations in *KCNJ1* may be a crucial determinant of the severity of the phenotype. However, examination of more patients are needed before a reliable correlation between genotype and phenotype can be established.

It is interesting to note that the majority of the core region mutations exerted a dominant negative effect, demonstrating that the mutant channels are synthesized and capable for oligomerization. In the tetrameric assembly of ROMK, one mutated subunit may be sufficient to impair channel function. This is in accordance with functional data obtained from ROMK1 core region deletion mutants [27]. Statistically, assuming a 1:1 stoichiometry of mutant and wild-type subunits, only 1 out of 16 tetrameric channels should be composed of four wild-type subunits. This ratio may be too low to maintain a physiologically relevant K^+ conductance in the TAL. Genetically, however, transmission of HPS/aBS is recessive, and heterozygous carriers of ROMK mutations do not suffer from the disease. This discrepancy might be explained by up-regulated transcription of wild-type alleles or the ability of wild-type ROMK subunits to form heterotetramers with other members of the Kir family, such as Kir4.1 and Kir4.2 [11, 12].

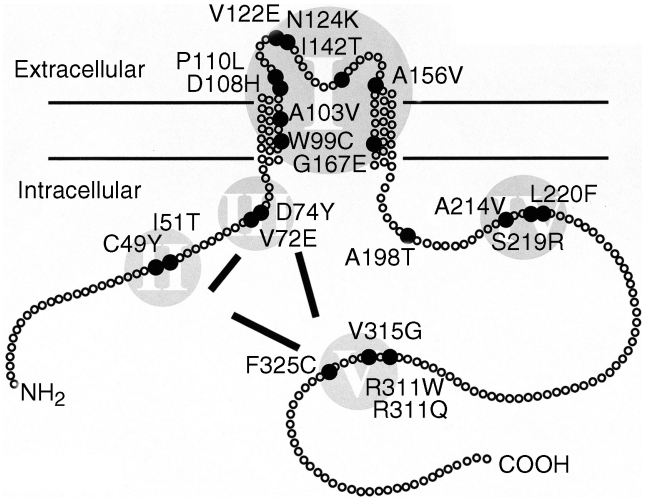

Fig. 5. Distribution and clustering of missense mutations in the ROMK channel molecule. Residues changed in HPS/aBS patients are indicated by filled circles (●). Mutations are grouped in clusters I-V, which contribute to distinct biophysical properties of the channel molecule. The lines between clusters II, IV, and V indicate putative interactions between the residues responsible for pH-dependent gating.

Only the W99C mutant showed a significant increase in macroscopic current when coexpressed with wild-type subunits. Two explanations are possible: (*1*) Mutant and wild-type assemble and tetrameric channels containing one or more W99C subunits are functional to certain extent (partial rescue), and/or (*2*) oligomerization between wild-type and W99C subunits is impaired, resulting in a significantly higher amount of "pure" wild-type tetramers than assumed by a 1:1 stoichiometry.

Together with the two novel pore mutations, 21 different missense mutations have been described to date, distributed throughout the channel protein (Fig. 5). They are tentatively grouped in five clusters: (*1*) within the channel core region (aa 84-180), (*2*) in the cytosolic N-terminal domain (aa 40-60), (*3*) nearby lysine-80 (aa 70-80), (*4*) in the ATP-binding regulatory domain (aa 190 to 240) C-terminal to M2, and (*5*) in the C terminus around R311. Mutations in the core region reduces K^+ conductance to a various extent, as demonstrated in this study. The majority of mutations in clusters (*2*), (*3*), and (*5*) have been argued to change the structural arrangement of the pH sensor and shift the pH gating to more alkaline pH values [15]. Mutations in cluster (*4*) may abolish PKA phosphorylation, which was found to lower

the affinity for phosphatidylinositol lipids [28] and thus may account for a decline of channel open probability [18]. Moreover, it has been demonstrated that removal of target sites for PKA (for example, S219) shifted pH gating off the physiological range [15], thus establishing a common pathogenic principle among the four intracellular clusters.

In contrast to the missense mutations, the C-terminal frameshift mutation (H354fs) resulted in macroscopic currents with amplitudes comparable to wild-type ROMK and virtually unaffected biophysical properties. We speculate that other mechanisms, for example, incorrect targeting to the apical membrane in epithelial cells or incompatibility with interaction partners, such as CFTR and other Kir subunits, are responsible for the HPS/aBS phenotype. In Kir2.3 channels, transfected into polarized MDCK cells, removal of the extreme C-terminus, which contains a consensus sequence for PDZ protein binding, caused mistargeting of the channel to the opposite membrane (abstract; *The Physiologist* 42:A18, 1999). In ROMK channels, the role of the putative PDZ binding-motif (TKM-Stop) has not yet been analyzed. Interestingly, a recent report showed that removal of the C-terminus at position aa331, also linked to HPS/aBS, resulted in a nonconductive channel [29]. Incremental reconstruction of the C-terminus delimited aa332-351 as the critical residues for restoring channel activity.

Finally, mutations outside the *KCNJ1* coding region are of particular interest because they may provide insights into the physiological role of ROMK isoforms. Both patients IX and X carry a deletion of at least 1100 bp, including putative transcription initiation sites (*TATA* box and a *CAAT* promoter box) 5′ of exon 1 [30]. These promoter elements are utilized by ROMK isoforms 2 and 3, whereas transcription of ROMK1 is likely initiated by a second promoter 5′ of exon 4, independent from an additional upstream promoter (Fig. 2). Even though both patients are expected to express ROMK1 correctly, they developed a severe TAL disorder. This may be due to the differential expression of the ROMK isoforms along the nephron demonstrated in rat, with ROMK2 and ROMK3 expressed in the TAL and ROMK1 expressed in the cortical collecting duct only [5]. Transferring this expression pattern to humans, one might expect that ROMK1 predominantly participates in net K^+ secretion in the distal nephron. Indeed, most of the patients with inactivating mutations affecting all ROMK isoforms had transient hyperkalemia (mean 6.8 ± 1.8 mmol/L) in the neonatal period, most likely because of defective cortical collecting duct (CCD). The absence of hyperkalemia in patients IX and X, however, is consistent with preservation of the K^+ secretion pathway via ROMK1 in these subjects. During follow-up, patients with functional ROMK1 might be prone to develop more severe hypokalemia. We could not test this hypothesis because both patients were diagnosed very early, and appropriate treatment with indomethacin and potassium supplementation, respectively, was introduced from that time on. The data from rats further suggest that ROMK2 and ROMK3 specifically mediate K^+ recycling in the TAL, ensuring that an adequate supply of luminal potassium is provided for efficient function of the Na-K-2Cl cotransporter. Again, this is consistent with the patients' clinical presentation, including saliuretic polyuria and hypercalciuria as a consequence of defective NaCl reabsorption in the TAL.

Various ROMK mutations affect residues critical for channel function, some of them related to previously recognized channel properties, others revealing new aspects of channel function and regulation. The combination of mutations in compound heterozygous subjects may not be arbitrary, but rather follow principles related to the tertiary or quaternary structure of the protein. A frequent dominant-negative effect of ROMK mutations, resulting in a loss-of-function, is based on the tetrameric assembly of the ROMK protein. A major challenge for future work in this field is to develop therapies directed at the restoration of channel function by targeting the underlying molecular defect.

ACKNOWLEDGMENTS

This work was supported by Deutsche Forschungsgemeinschaft (Se 263/15-1, Ko 1480/3-2, Da 177/7-3) and Forschungspool FB20 of the Philipps-University Marburg. A preliminary account of this work was presented at the 1999 APS Conference *Biology of Potassium Channels: From Molecules to Disease*, Snowmass Resort, Colorado, USA. We thank Dr. E. Wingen, Dr. M. Boeswald, Professor Dr. P. Koepp, Dr. J. Matyas, and Dr. H. Kalhoff for the contribution of patients and data collection.

Reprint requests to Martin Konrad, M.D., Department of Pediatrics, Philipps-University, Deutschhausstrasse 12, D-35037 Marburg, Germany.
E-mail: konradm@mailer.uni-marburg.de

REFERENCES

1. Giebisch G: Renal potassium transport: Mechanism and regulation. *Am J Physiol* 274:F817–F833, 1998
2. Greger R: Ion transport mechanisms in thick ascending limb of Henle's loop of mammalian nephron. *Physiol Rev* 65:760–797, 1985
3. Ho K, Nichols CG, Lederer WJ, *et al:* Cloning and expression of an inwardly rectifying ATP-regulated potassium channel. *Nature* 362:31–38, 1993
4. Shuck ME, Bock J, Benjamin C, *et al:* Cloning and characterization of multiple forms of the human kidney ROM-K potassium channel. *J Biol Chem* 269:24261–24270, 1994
5. Boim MA, Ho K, Shuck ME, *et al:* ROMK inwardly rectifying ATP-sensitive K^+ channel: Cloning and distribution of alternative forms. *Am J Physiol* 268:F1132–F1140, 1995
6. Simon DB, Karet FE, Rodriguez-Soriano J, *et al:* Genetic heterogeneity of Bartter's syndrome revealed by mutations in the K^+ channel, ROMK. *Nat Genet* 14:152–156, 1996
7. International Collaborative Study Group for Bartter-Like Syndromes: Mutations in the gene encoding the inwardly-rectifying renal potassium channel, ROMK, cause the antenatal variant of Bartter syndrome: Evidence for genetic heterogeneity. *Hum Mol Genet* 6:17–26, 1997

8. McCredie DA, Rotenberg E, Williams AL: Hypercalciuria in potassium-losing nephropathy: A variant of Bartter's syndrome. *Aust Paediatr J* 10:286–295, 1974
9. Seyberth HW, Rascher W, Schweer H, *et al:* Congenital hypokalemia with hypercalciuria in preterm infants: A hyperprostaglandinuric tubular syndrome different from Bartter syndrome. *J Pediatr* 107:694–701, 1985
10. Doupnik CA, Davidson N, Lester HA: The inward rectifier potassium channel family. *Curr Opin Neurobiol* 5:268–277, 1995
11. Shuck ME, Piser TM, Bock JH, *et al:* Cloning and characterization of two K^+ inward rectifier (Kir) 1.1 potassium channel homologs from human kidney (Kir1.2 and Kir1.3). *J Biol Chem* 272:586–593, 1997
12. Derst C, Wischmeyer E, Preisig-Müller R, *et al:* A hyperprostaglandin E syndrome mutation in Kir1.1 (renal outer medullary potassium) channels reveals a crucial residue for channel function in Kir1.3 channels. *J Biol Chem* 273:23884–23891, 1998
13. McNicholas CM, Guggino WB, Schwiebert EM, *et al:* Sensitivity of a K^+ channel (ROMK2) to the inhibitory sulfonylurea compound glibenclamide is enhanced by coexpression with the ATP-binding cassette transporter cystic fibrosis transmembrane regulator. *Proc Natl Acad Sci USA* 93:8083–8088, 1996
14. Wang W, Schwab A, Giebisch G: Regulation of small-conductance K^+ channel in apical membrane of rat cortical collecting tubule. *Am J Physiol* 259:F494–F502, 1990
15. Schulte U, Hahn H, Konrad M, *et al:* pH-gating of ROMK ($K_{ir}1.1$) channels: Control by an Arg-Lys-Arg-triad disrupted in antenatal Bartter syndrome. *Proc Nat Acad Sci USA* 96:15298–15303, 1999
16. Derst C, Konrad M, Köckerling A, *et al:* Mutations in the ROMK gene in antenatal Bartter syndrome are associated with impaired K^+ channel function. *Biochem Biophys Res Commun* 230:641–645, 1997
17. Schwalbe R, Bianchi L, Accili EA, Brown A: Functional consequences of ROMK mutants linked to antenatal Bartter's syndrome and implications for treatment. *Hum Mol Genet* 7:975–980, 1998
18. MacGregor GG, Xu JZ, McNicholas CM, *et al:* Partially active channels produced by PKA site mutation of the cloned renal K^+ channel, ROMK2 (Kir1.2). *Am J Physiol* 275:F415–F422, 1998
19. Maniatis T, Fritsch EF, Sambrook J: *Molecular Cloning: A Laboratory Manual* (2nd ed). Cold Spring Harbour, Cold Spring Harbour Laboratory, 1987
20. Orita M, Suzuki YH, Sakiya T, Hayaski K: Rapid and sensitive detection of point mutations and DNA polymorphisms using the polymerase chain reaction. *Genomics* 5:874–879, 1989
21. Taugner R, Waldherr R, Seyberth HW, *et al:* The juxtaglomerular apparatus in Bartter's syndrome and related tubulopathies: An immunocytochemical and electron microscopic study. *Virchows Arch A Pathol Anat Histopathol* 412:459–470, 1988
22. Köckerling A, Reinalter SC, Seyberth HW: Impaired response to furosemide in hyperprostaglandin E syndrome: Evidence for a tubular defect in the loop of Henle. *J Pediatr* 129:519–528, 1996
23. Feldmann D, Alessandri JL, Deschenes G: Large deletion of the 5′ end of the ROMK1 gene causes antenatal Bartter syndrome. *J Am Soc Nephrol* 9:2357–2359, 1998
24. Pessia M, Tucker SJ, Lee K, *et al:* Subunit positional effects revealed by novel heteromeric inwardly rectifying K^+ channels. *EMBO J* 15:2980–2987, 1996
25. Pearson WL, Dourado M, Schreiber M, *et al:* Expression of a functional Kir4 family inward rectifier K^+ channel from a gene cloned from mouse liver. *J Physiol* 514:639–653, 1999
26. Doyle DA, Morais Cabral J, Pfuetzner RA, *et al:* The structure of the potassium channel: Molecular basis of K^+ conduction and selectivity. *Science* 280:69–76, 1999
27. Koster JC, Bentle KA, Nichols CG, Ho K: Assembly of ROMK1 (Kir1.1a) inward rectifier K^+ channel subunits involves multiple interaction sites. *Biophys J* 74:1821–1829, 1998
28. Liou HH, Zhou SS, Huang CL: Regulation of ROMK1 channel by protein kinase A via a phosphatidylinositol 4,5-bisphosphate-dependent mechanism. *Proc Natl Acad Sci USA* 96:5820–5825, 1999
29. Flagg TP, Tate M, Merot J, Welling PA: A mutation linked with Bartter's syndrome locks Kir 1.1a (ROMK1) channels in a closed state. *J Gen Physiol* 114:685–700, 1999
30. Bock JH, Shuck ME, Benjamin CW, *et al:* Nucleotide sequence analysis of the human KCNJ1 potassium channel locus. *Gene* 188: 9–16, 1997